Thermal And Near infrared Sensor for carbon Observation (TANSO)
on board
the Greenhouse gases Observing SATellite (GOSAT)

Research Announcement

Appendix B

GOSAT/TANSO Calibration and Validation Plan and Overview of Processing Algorithms

B-1 GOSAT/TANSO Calibration Plan

B-1.1 Outline

"Calibration" is an evaluation process to clearly characterize the sensor and to ensure that the accuracies of radiance, geometry, spectral characteristics, image quality, etc. meet the target values, using Level 1 (L1) products out of the standard products. The specific methods of evaluation include:

- Evaluation of performance in ground tests (before the launch, using ground test data)
- In-orbit calibration (after the launch, using cal-mode data), and
- Vicarious calibration (after the launch, using actual observation data, etc.)

Based on the results of these calibration activities, L1 products will constantly be upgraded by reflecting the revised calibration coefficients and the corrected L1 processing algorithm in the ground processing system.

B-1.2 Calibration Schedule

The evaluation of the sensor performance on the ground will be completed by approximately one year before the launch. The initial in-flight calibration will be carried out during the operational phase, between three and six months after the launch. The calibrated Level 1 products will be released as Version 1, expectedly within six months from the launch. Thus, the data to be collected and examined during the initial calibration period only covers a period of less than a year, and it is important to thoroughly examine match-up conditions, etc. for data acquisition during this period.

B-1.3 Pre-launch Performance Test

The main functions and capabilities of TANSO-FTS and TANSO-CAI will be evaluated before the launch. The evaluation is basically conducted by checking the following items in ground tests.

(1) Sensitivity and signal-to-noise ratio (SNR)
The sensitivities of FTS at short wavelength infrared bands and CAI, an indicator for the photoelectric conversion efficiency, and SNR are calibrated and evaluated by using an evaluated integrating sphere. The evaluation of the integrating sphere is carried out by using a comparative spectrometer in comparison with a fixed point blackbody furnace coated with such material as zinc. The sensitivity calibration for FTS thermal infrared (TIR) band and SNR evaluation are performed by using a blackbody cavity at the thermal vacuum test.

(2) Polarization sensitivity
The polarization sensitivity of FTS at short wavelength infrared bands and CAI will be carried out in the following steps: i) install a polarizer at the exit port of the integrating sphere to form linearly polarized light, ii) rotate the phase of the linearly polarized light by rotating the 1/2 wavelength plate attached behind, and iii) introduce rotating linearly polarized light so as to

obtain the polarization sensitivity. In case of TANSO-FTS, the incoming light is polarized mainly at the reflector of the pointing mechanism and the beam splitter of the Fourier interferometer mechanism.

(3) Instrument function
FTS's instrument function serves as an indicator for the spectral resolution. The function is obtained by introducing diffused light from a tunable laser for each band. As for CAI, the spectral characteristics are obtained by introducing monochromatic light.

(4) Field of View (FOV) and Modulation Transfer Function (MTF)
The FOVs of FTS and CAI, which serve as indicators for optical capabilities, and the MTF of CAI are evaluated by setting up a point light source and a slit light source at the collimator. The alignment to the sensor reference axis and band-to-band/pixel-to-pixel alignment are also evaluated at the same time.

In addition, FTS is equipped with a high-resolution monitoring camera (CAM) to check its FOV. The CAM has the same look direction as FTS. The alignment of the CAM to the sensor reference axis will also be evaluated.

B-1.4 Post-launch calibration
Calibrations after the launch will be carried out in two modes: in-orbit calibration and vicarious calibration. The former is performed on the calibration mode data, whereas the latter uses actual observation data.

The cal-mode data acquired during in-orbit calibration are precisely defined in Chapter C-2.4.3 "Operation in the calibration mode" of Appendix C "Operation Policies of GOSAT and Basic Observation Plan of the TANSO Sensor". The cal-mode data are acquired in accordance with the operation policies provided thereof and used for L1 processing, trend evaluation, etc.

B-1.4.1 Calibration of the TANSO-FTS (short wavelength infrared (SWIR) bands)

The in-flight calibration of TANSO-FTS will be carried out in three aspects: radiance, geometry and spectral characteristics. The following items will be evaluated with respect to each of P and S polarization bands in short wavelength infrared (SWIR) bands (Bands 1-3).

(1) Radiance evaluation
  (a) Calibration of the sensitivity
  In-orbit calibration of SWIR bands will be performed through solar irradiation calibration using the diffuser plate for every orbit, and deep-space calibration in parallel with TIR band is performed. In L1 processing, it is planned to convert the observed values into radiance values using the sensitivity calibration coefficients obtained from ground tests. The coefficients will be revised based on an analysis of the results from the solar irradiance calibrations, lunar calibrations (to be discussed in more details later), and vicarious calibrations.

(b) Lunar calibration

The purpose of lunar calibration is to calibrate the efficiency of the overall optical system for SWIR bands by using the reflected solar radiation from the moon surface as the calibration source. The lunar calibration will be performed on the orbit when the average of lunar surface radiance becomes the largest (at lunar age of 14.8±0.1). In this calibration, the satellite will be oriented to the moon so that FTS's FOV catches the moon on the full scale, and FTS will keep pointing at the moon with its pointing mechanism for at least two minutes.

The moon is an extremely stable reflector with a radiance variance of 10^{-7}/year. The stability has been reported so high that the fluctuation is less than 1%, based on the results from the sensitivity trend evaluations for those sensors observing ultra violet to short wavelength infrared bands, such as MODIS, ASTER, etc., that have been conducted as part of lunar calibrations (USGS, 2006). The evaluation methods adopted in these past evaluations are as follows:

- The sensitivity trend was evaluated at each time of calibration using a stable light source.
- The absolute sensitivity was evaluated based on ROLO data—ROLO (RObotic Lunar Observatory) is USGS's reflectance database for lunar calibration.

(c) Linearity

The linearity for the response of the optical system, including temperature dependence, will be checked based on the data observed while uniform light with different radiance levels is introduced into the FTS optical system. Listed below are candidate targets that have uniform radiances.

- Offset: Deep-space calibration
- Low radiance: Ocean, snow and ice (B2-3)
- Medium radiance: Forestry
- High radiance: Solar irradiation calibration, snow and ice (for B1 only), dry salt lakes (for B1 only), desert, playa

(d) Absolute radiance

The radiance observed by FTS is compared with the radiance of ground surface radiation obtained from the experiments in vicarious calibrations or synchronous observations with a well-calibrated sensor on board other spacecraft or aircraft. In order to match the radiances of the reference instrument and FTS, the sensor radiance model, and calibration coefficients are adjusted and absolute radiometric accuracies are evaluated.

There are two major approaches to this evaluation method:

- To use in-situ data
- To use global data

(i) Using in-situ data

Specific physical parameters, such as the ground-surface reflectance, as to a

specific location on the earth are obtained accurately and synchronously in a vicarious calibration experiment. The GOSAT-observed radiance is evaluated in comparison with the radiance at the top of atmosphere computed by using the above mentioned parameters. Since the observation bands contain absorption bands of CO_2, CH_4 and other species, it is desirable to synchronize the validation experiments with this evaluation.

(ii) Using global data

The synchronized data are extracted from the data acquired by a well-calibrated sensor on board other spacecraft for radiance comparison. Since the radiance is influenced by the observation timing or geometry, the FTS data and the reference data may not easily fit when directly compared. In such a case, the radiance is evaluated by comparing the GOSAT-observed radiance with the radiance at the top of atmosphere computed based on the physical parameters, such as ground-surface reflectance.

Currently, Aqua/MODIS and OCO (Orbiting Carbon Observatory) are listed as candidates for reference satellites in this comparative evaluation.

(e) Relative radiance between the sensors

FTS and CAI both observe the 1.6μm band in Bands 2 and 4, respectively. The relative radiance accuracy between the two sensors is evaluated by assessing the temporal variation and temperature dependence per gain.

(2) Geometric evaluation

(a) Pointing accuracy

The alignment of the CAM, attached in the FTS sensor for checking its FOV, and FTS is assumed to be known and the CAM has an FOV of approximately 30 km and a spatial resolution of approximately 100 m in the VGA mode. FTS's geometric accuracy is evaluated using imagery taken by the CAM over GCPs with known coordinates as well as clear radiance boundaries between bright and dark. The following scenes are to be used in this evaluation:

- Land/sea boundaries (scenes containing coastal lines also covering projections from the land, such as peninsulas and capes)
- Islands (scenes containing the whole land of an island within the FTS's FOV of 10 km)

(b) Pointing stability

The pointing accuracy of the pointing mirror during an interferogram measurement (typically for four seconds) is evaluated by acquiring data by the CAM in the movie mode. The following scenes are to be used in this evaluation:

- Land/sea boundaries (scenes containing coastal lines also covering projections from the land, such as peninsulas and capes)

(c) Geometric accuracy between the sensors

The geometric accuracy between FTS and CAI is evaluated by assessing the displacements of common GCPs on CAM and CAI images. Further, since the sensors observe the same wavelength region, the geometric accuracy of FTS can be comparatively assessed against CAI by searching the position of FTS Band 2 (10-km resolution) on a CAI Band 4 (1.5-km resolution) image with the radiance matching function.

(3) Evaluation of spectral characteristics

(a) Instrument function

The instrument function of Band 2 is evaluated by irradiating 1.55μm semiconductor laser light onto the diffuser plate and observing the diffused light.

(b) Wavelength accuracy

The wavelength shift is evaluated by referring to the wavelength position of a known atmospheric absorption band.

(c) Polarization sensitivity

The radiance ratio between the P and S polarization bands of the target with known polarization characteristics is evaluated using the following data.

・Solar irradiation calibration data (natural light of the sun is unpolarized.)

(d) SNR

Targeting a uniform high-radiance range, the SNR is evaluated as to each band detector and gain. The following data will be accumulated and used for the evaluation.

・ Solar irradiation calibration data
・ Desert, snow and ice (for B1 only)

B-1.4.2 Calibration of TANSO-FTS (TIR band)

(1) Radiance evaluation

(a) Calibration of the sensitivity

In-orbit calibration of TIR band will be performed using deep-space radiation (equivalent to a radiance temperature of 3 K) and the blackbody on board the satellite (equivalent to a radiance temperature of app. 290 K). The L1 processing algorithm for this calibration is currently assumed to employ the following methods:

・ The blackbody and deep-space radiances are assigned to the highest level and the lowest level, respectively, for fitting based on a high-order regression curve. The values obtained in the ground tests are used as the factors in the high-order terms.
・ Since the sensitivity is subject to the influence of background radiances inside the instrument, phase correction should be taken into consideration, while at the same time directing attention to the combination of data to be used in the calibration, the monitored temperature of the sensor, etc.

(b) Linearity

The offset and linearity of the response of the optical system, including temperature dependence, will be checked based on the observation data taken while uniform light with different radiance levels is introduced into the FTS optical system. The following lists up candidate data to be used for this evaluation.

- Offset: Deep-space calibration
- Low radiance: Snow and ice
- Medium radiance: Forestry, oceanography
- High radiance: Blackbody calibration, deserts, playa

(c) Absolute radiance

Similarly to SWIR bands, the absolute radiance of TIR band will be evaluated by the following two approaches:

- To use in-situ data
- To use global data

(i) Using in-situ data

A high-accuracy calibration will be performed by acquiring the atmospheric profile, including temperature of air, water vapor, etc., while targeting the locations where the sea surface temperature is measured with buoys.

(ii) Using global data

The synchronized data are extracted from the data (equivalent to Level 1) acquired by a well-calibrated sensor on board other spacecraft for radiance comparison. Furthermore, the accuracy of calibration is evaluated over a wide area of the ocean by using sea-surface temperature and meteorological data on the global scale with a high, consistent accuracy.

Currently, Aura/TES and Aqua/AIRS are listed as candidates for reference satellites in this comparative evaluation, and NOAA's sea-surface temperature (SST) analysis of Reynolds, etc. are planned for the reference database.

(2) Geometric evaluation

Since the same optical system is used for acquiring FTS SWIR and TIR band data, the geometric evaluation of TIR band is conducted following that of SWIR bands.

(3) Evaluation of spectral characteristics

(a) Wavelength calibration

The wavelength shift is evaluated by observing known atmospheric absorption bands.

(b) SNR

Targeting a uniform high-radiance range, the SNR is evaluated as to each gain. The following data will be accumulated and used for the evaluation.

- Blackbody calibration
- Desert

B-1.5 Calibration of TANSO-CAI

(1) Radiance evaluation

(a) Calibration of the sensitivity

CAI does not carry any special functions associated with the sensitivity calibration in orbit. Thus, the calibration is performed only with the sensitivity calibration expression to be obtained in the ground tests. However, the following data will be acquired as solely for the offset (dark signal output).

- Nighttime observation
- Optical black element

(b) Lunar calibration

The lunar calibration for CAI will be performed on the same orbit as that of FTS. It is intended to calibrate the sensitivity of the devices of the linear array detectors where lunar calibration light enters. In this calibration, CAI imagery will be acquired while scanning an area of ±2.55deg or greater covering the entire moon surface twice in both ways (four scans) continuously at an angular velocity of 0.1 deg/sec or less in the Y-axis direction.

(c) Linearity

The linearity of the response of the optical system, including temperature dependence, is evaluated based on the observation data taken while uniform light with different radiance levels is introduced to the CAI optical system. Listed below are candidate targets that have uniform radiances.

- Offset: Nighttime observation, optical black element
- Low radiance: Ocean, snow and ice (for B4 only)
- Medium radiance: Forestry
- High radiance: Snow and ice (B1-3), dry salt lakes (B1-3), desert, playa

(d) Absolute radiance

Similarly to FTS, the absolute radiance of CAI will be evaluated by the following two approaches:

- To use in-situ data
- To use global data

(i) Using in-situ data

The calibration coefficients are determined through optimization based on aerosol data measured at as many locations as possible by the AERONET (NASA, 2006) and SKYNET (Chiba Univ., 2006), both of which are deployed worldwide.

(ii) Using global data

The synchronized data are extracted from the data (equivalent to Level 1) acquired by a well-calibrated sensor on board other spacecraft for radiance comparison. Furthermore, the accuracy of calibration is evaluated by using the ground surface reflectance, aerosol parameters, climatological values, and other physical values (equivalent to Level 2) or

databases providing these values, acquired by other spacecraft on the global scale with a high, consistent accuracy.

Currently, Aqua/MODIS and Aura/OMI are listed as candidates for reference satellites in this comparative evaluation, and the ground surface reflectance datasets of GOME (Global Ozone Monitoring Experiment) and TOMS (Total Ozone Mapping Spectrometer), etc. are planned for the reference database.

(2) Geometric evaluation

(a) Pointing accuracy

The geometric accuracy of CAI imagery is evaluated using imagery taken over GCPs with known coordinates as well as clear radiance boundaries between bright and dark.
The GCP database to be used for GOSAT should be chosen beforehand from coastline database GSHHS.
The following scenes are to be used in this evaluation:

- Land/sea boundaries (scenes containing coastal lines also covering projections from the land, such as peninsulas and capes)

(b) Band-to-band registration

The offset between bands is determined relatively by evaluating the pointing accuracy as to each band, as described in (a) above.

(3) Image quality evaluation

(a) Calibration of the pixel-to-pixel sensitivity

The coefficients for correcting the pixel-to-pixel sensitivity are calculated by accumulating data in each pixel direction, deriving the average values, and comparing the averages in the line direction, using data taken over wide-area targets with uniform, high radiances. Since GOSAT's swath stretches for 750-1,000 km, it is infeasible to perform the calibration at once. Thus, more than one site must be selected for the calibration. The following lists up the candidate target sites.

- Snow and ice (B1-B3), desert

(b) MTF

In order to extract edge and point spectra, the MTF is calculated using geometrically-corrected observation data covering edges, such as coastal lines, and point sources, such as islands. Based on the derived MTF, the spatial resolution dependent on the optical characteristics is evaluated. The following scenes are to be used in this evaluation:

- Coastal lines
- Islands

(c) SNR

Targeting a uniform high radiance range, the SNR is evaluated as to each band detector

and gain. The following data will be accumulated and used for the evaluation.

- Snow and ice (B1-3), dry salt lakes (B1-3), desert, playa

B-1.6 Preparation for Calibration

(1) Examination of the calibration approach with the use of in-situ data

In vicarious calibrations using TANSO observation data and ground observation data, it is important to select test sites in view of the uniformity (across the FTS's FOV of 10 km), temporal stability, probability of clear sky, and accessibility. The following candidate sites have been found as satisfactory for the calibration purpose.

- Railroad Valley Playa, Nevada, U.S.A.
- Strzelecki Desert (Tinga Tingana), South Australia, Australia

These sites have been scrutinized in terms of appropriateness as the calibration sites. Railroad Valley has constantly been used as a vicarious calibration site for Landsat, MODIS, ASTER, etc. by the University of Arizona for a long time. The OCO project likewise is considering the use of the valley as its calibration test site. Tinga Tingana in Strzelecki Desert is a highly uniform site where the CSIRO (Commonwealth Scientific and Industrial Research Organisation) of Australia has set up a part of the AERONET.

Figure B-1-1 below shows MODIS images over Railroad Valley and Tinga Tingana. The red circles indicate the FTS's FOV of 10 km when it is pointing at the sites. Each image stretches for 30 km×30 km. While the uniform area in Railroad Valley just barely covers the 10-km FOV of FTS, Tinga Tingana is covered with uniform land that amply extends over the FOV. Figure B-1-2 plots the probability of clear sky throughout 2004 at these sites, and the graph apparently suggests that the probability drops during wintertime at both sites. Thus, it is desirable to secure calibration sites in both north and south hemispheres in consideration of the launch schedule. It is still under examination whether these sites are selected for GOSAT's calibration sites or not.

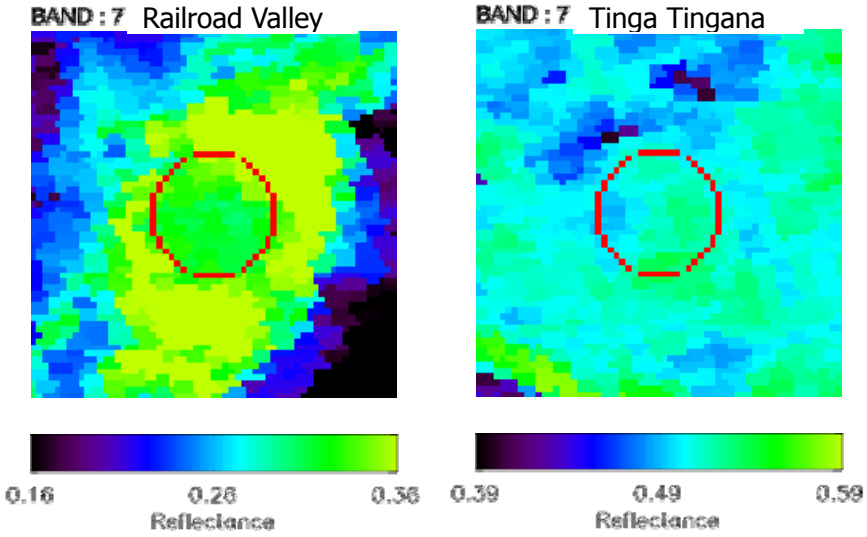

Figure B-1-1 MODIS band 7 (2.1μm) images over the candidate calibration sites

(2) Examination of the calibration approach with the use of global data

In order to select most appropriate sites for cross-calibration with data taken by other missions, the spatial uniformity, temporal stability, etc. at the candidate sites are evaluated based on the existing global data observing these sites.

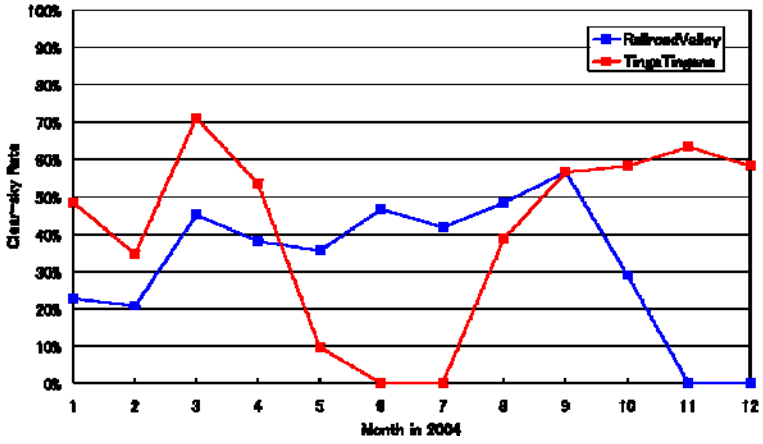

Figure B-1-2 Clear-sky rate at the candidate calibration sites
(Aqua/MODIS data in 2004)

Figure B-1-3 indicates an average reflectance distribution on the 5 x 5 pixel basis (app. 25 square kilometers) of MODIS band 7 (2.1μm) data and the standard deviation among 25 samples. The samples were retrieved from the global reflectance data (average of 16 days) of MODIS on board Aqua and Terra. There are several spots with uniform reflectance in the Sahara Desert and the Rub' al khali Desert. In addition, as the reflectance in this band is susceptible to soil moist and decreases with it, a high reflectance is obtained only in deserts or bare lands.

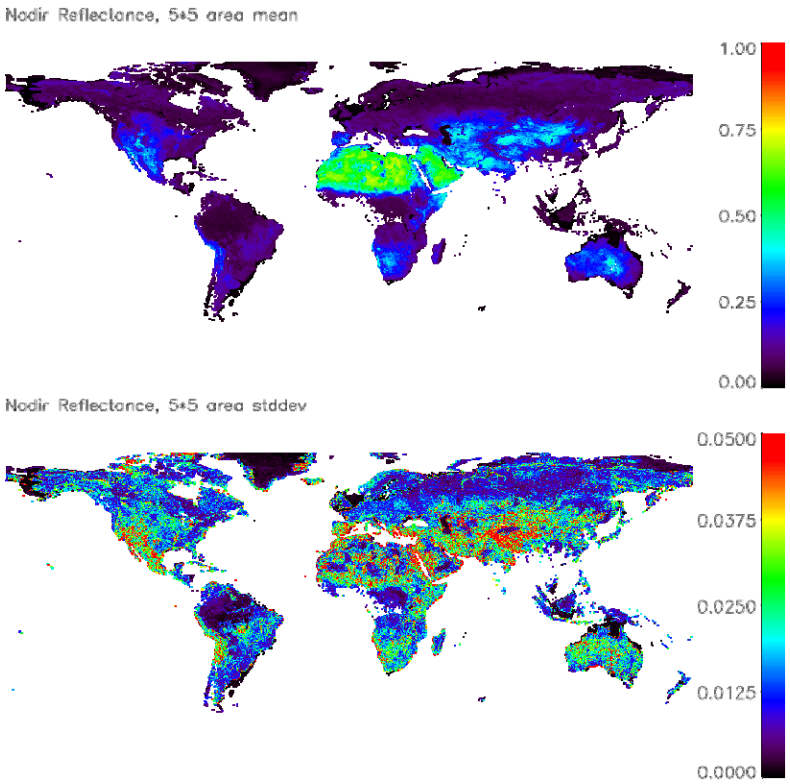

Figure B-1-3 Survey on the spatial uniformity using the ground surface reflectance data acquired by MODIS band 7 (2.1μm)
Upper: Average reflectance of 5×5 pixels (app. 25km)
Lower: Standard deviation of 25 samples

Figure B-1-4 shows an annual average of the ground surface reflectance in the Sahara Desert (of app. 22 samples), and the standard deviation for the year. POLDER (POLarization and Directionality of the Earth's Reflectances) targeted the sites marked with x, namely Egypt 1 (N27.12, E26.10) and Algeria 3 (N30.32, E7.66), in its vicarious calibration. (Hagolle, 1999) Figure B-1-5 plots the reflectance at Egypt 1 and Algeria 3 during the year in the time series. It reveals that those sites selected by POLDER have a high temporal stability and, as shown in Figure B-1-3, a high spatial uniformity.

Based on the analyses of these existing data, the GOSAT Project will select the most appropriate sites for its calibration activities in light of the resolutions and swaths of TANSO-FTS and CAI, and collect data accordingly.

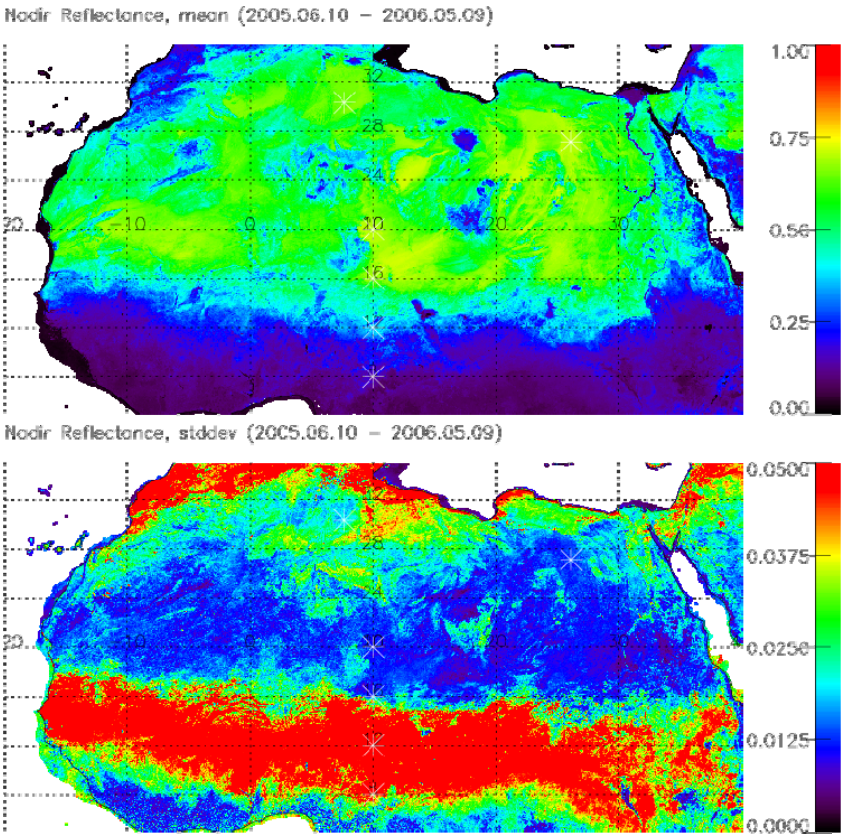

Figure B-1-4 Investigation on the temporal stability based on the ground-surface reflectance data of MODIS band 7 (2.1μm)
Upper: Annual average (app. 22 samples)
Lower: Standard deviation

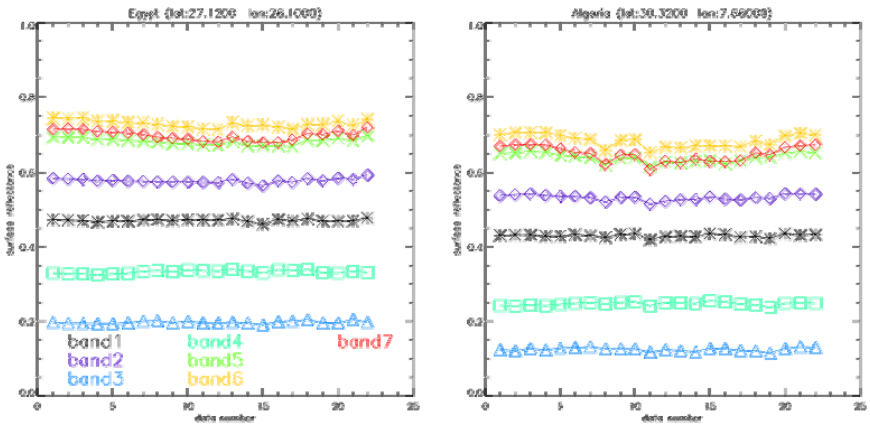

Figure B-1-5 Chronological plotting of the ground-surface reflectance at the specific observation points for one year
Left: Egypt 1 site Right: Algeria 3 site

B-2 GOSAT/TANSO Validation Plan

B-2.1 Basic philosophy for the validation

"Validation" of GOSAT products means an evaluation of uncertainties of GOSAT L2, L3 and L4 products, as provided in Table 1 of the Research Announcement document*, compared with other data with less uncertainties that were acquired independently of GOSAT. "Comparison", on the other hand, means an evaluation of uncertainties of GOSAT products against observation data with equivalent uncertainties or data estimated by simulation models; thus it should be distinguished from "validation" above. Both evaluation methods, however, are intended to assess the data quality of GOSAT products (data quality assurance), and at the same time play a significant role in evaluating the appropriateness of the data processing algorithms. Therefore, any findings from the evaluations will be reflected in revising the algorithms, as necessary.

Additionally, the "calibration" is an evaluation of L1 product data to be performed mainly by JAXA and focuses on calibration of radiance spectra (e.g., absolute radiance, linearity, offset, wavelength, instrument function, SNR, etc.) However, it excludes an evaluation of spectral parameters and the Fraunhofer lines, which are necessary for retrieval of the CO_2 and CH_4 column abundances based on the radiance spectra obtained from TANSO-FTS observation data, since these values have been evaluated at the algorithm development stage.

In formulating a validation plan for GOSAT TANSO, it is important first to assign priority orders to the validation items because the manpower and budget for observation and analysis activities in connection with the validation are not unlimited.

The appropriateness of the processing algorithms must be verified prior to the launch of the satellite. This evaluation is called "algorithm validation". The algorithm validation has been conducted through observational experiments by the FTS sensor installed at a high elevation and on an aircraft. These observational experiments must continually be performed in the future to improve the algorithms.

After launch, another important evaluation, in addition to product validation, is to verify the appropriateness of parameters, such as optical characteristics of aerosols, which are relevant to errors. This post-launch evaluation is called "parameter validation". Although GOSAT makes greater social contribution with its higher-level products than lower-level products (L2), validation of the latter is of primary importance as it provides the foundation for generating the former. Thus, it is preferred to perform validation of lower-level products first followed by that of higher-level products.

The priorities of GOSAT product validation and comparison have been set as follows:

(1) L2 SWIR CO_2 and L2 SWIR CH_4 column abundances
(2) L2 TIR CO_2 and L2 TIR CH_4 vertical profile of concentration
(3) Global distributions of L3 SWIR CO_2 and CH_4 column abundances
(4) Global distribution of L4A CO_2 flux
(5) Global distribution of L4B CO_2 concentration

$$\left(\text{uncertainty} = \sqrt{(\text{accuracy})^2 + (\text{precision})^2} \quad \text{accuracy} = \text{bias} \right)$$

The basic policy on collection of validation data is to prioritize the use of diverse observation data being acquired routinely in all parts of the world, considering that the GOSAT itself observes the entire earth on varied conditions in terms of ground surface, meteorology, and atmosphere. To this end, certain specific observation points will be set as "super sites" for focused and continued observation for the validation purposes of products and algorithm, and necessary observing equipment are installed at these sites. Furthermore, campaign observations will be planned and carried out, which include air-borne observation on various meteorological conditions.

The data to be validated are those that have been taken on the following geographical and meteorological conditions:

a. Land area with clear sky
b. Sea area with clear sky (sunglint observation)
c. Land area with thin cirrus clouds and aerosols
d. Sea area with thin cirrus clouds and aerosols (sunglint observation)

*Excluding areas covered with thick clouds.

In addition, the validation must be conducted in light of certain standards for match-up conditions in terms of space and time.

Of all the analytical work in the validation, NIES will be responsible for the basic validations analysis and incorporation of the results into the revision of algorithms, as part of the GOSAT Project. In the meantime, it is expected that more research activities concerning the validation analysis of the GOSAT data products will be carried out by the GOSAT Science Team members, scientists participating in the RA, and other users at large.

B-2.2 Experimental observation for the algorithm validation

The processing algorithm to derive the CO_2 column abundance must be verified prior to the launch through experiments simulating the satellite observation geometry, more specifically, by observing solar light reflections from the earth surface with an FTS, a similar sensor to the one on board the satellite, installed at a high-elevation ground point or on board an airplane.

(1) Observation at a high elevation

NIES carried out two observational experiments using an FTS sensor, similar to TANSO-FTS, installed near the summit of Mt. Tsukuba Japan at an elevation of 800 m in 2005 and 2006. In these experiments, the CO_2 concentration calculated from the data acquired by FTS was compared with the measurement made by a light airplane, which took off from near the farmland close to the foot of the mountain and flew up to an altitude of 3,000 m carrying the CO_2 in-situ instrument. The results demonstrated an accuracy of about 1% of the FTS's observation with respect to the CO_2 column abundance in the atmospheric layers at an altitude of 3 km and lower. It is vital to continue observational experiment in this manner on various meteorological conditions in the future, pursuing

an improved accuracy.

(2) Air-borne observation

An algorithm validation is made by the spectroscopic observation using the FTS mounted on the aircraft at a very high altitude, simultaneously with the in-situ CO_2 concentration measurement onboard an aircraft. This method more directly simulates the behaviors of the FTS on board the satellite in nadir looking observation from a very high altitude than the observation at a high-elevation ground point, although the vibration of the aircraft remains as a problem.

B-2.3 SWIR/TIR Product Validation

(1) Validation of CO_2 and CH_4 column abundances by SWIR observation

The observing instrument to be used for validating the CO_2 and CH_4 column abundances must be based on fully-established technology with no bias, assuring data quality as well as achieving an excellent observation accuracy of about 1 %. An observation method which uses absorption of direct solar light is the best technique for observing the column abundance directly. Thus, a high-resolution FTS installed on the ground proves to be the most appropriate method among all available measuring instruments. FTS can observe spectrum anytime as long as there is direct solar irradiance for approximately 10 minutes.

The footprint of TANSO-FTS extends for as long as 10.5 km. In order to reduce observation errors, observation points where the surface cover is flat and uniform within this size are ideal for the purpose of the validation. Some of FTS's observation points are situated in mountainous areas; thus it is essential to collect surrounding information of the observation points and select flat areas that will least contribute to observation errors.

If there is an obvious bias in the TANSO-FTS retrieval results or if the measurement accuracy falls below a certain level, it is necessary to identify the cause of the error and improve the data processing algorithm. Of the various parameters that affect the retrieval of column abundances, namely cirrus cloud, aerosol, surface albedo, air pressure, air temperature, water vapor, and concentrations of other gases, the effects of cirrus cloud and aerosols are the most dominant. The surface albedo can be obtained fairly accurately from the TANSO-FTS observation data by means of a retrieval analysis and it does not substantially affect the derived column abundance value. Therefore, the priority of the surface albedo is set low. Furthermore, the priority of meteorological parameters, such as air pressure, air temperature, and water vapor, is also low since they are usually taken from meteorgical reanalysis data.

Measuring cirrus cloud and aerosol requires i) a sky radiometer that can estimate the optical thickness, the grain size distribution and the complex refraction index averaged in the nadir direction and ii) a polarized lidar that can identify the vertical distribution of cirrus clouds and aerosols and distinguish between sphericity and non-sphericity. Thus, it is important, in terms of validation strategy, to set up these instruments at the ground based FTS observation sites to enable simultaneous observation.

The vertical distribution data directly measured (sampled and analyzed) by a taking-off and landing

regular passenger airplane provide an effective reference for the derived CO_2 column abundance. However, this measurement can gather data for the vertical profile of CO_2 concentration between the ground level and an altitude of approximately 11 km. As about 22 % of CO_2 exists above the 11-km altitude, other methods to either correctly estimate or measure the CO_2 level above this altitude are needed for calculating the column abundance. If the fluctuation of CO_2 abundance in the higher altitudes remains within 4 %, the model climatological values derived from the past actual measurements can be used. Furthermore, CO_2 concentration on the ground surface needs to be measured in order to ascertain the concentration between the ground level and the minimum altitude where aircraft can measure. Moreover, it is desirable to use the sky radiometer and lidar in the vicinity of the validation sites for measuring cirrus cloud and aerosol. At some airports, however, the air is significantly contaminated. Therefore, meteorological conditions of the sites must be carefully examined when selecting validation sites.

As for CH_4, there is a possibility that air-borne observation (bottle sampling) data is effective. Moreover, it can be effective in validation as there are most recent data up to an altitude of about 35 km based on balloon observation.

Sunglint observation basically takes place on the ocean. However, validation of product by sunglint observation may be replaced by data acquired by a high-resolution FTS installed near coastal lines and/or data obtained by aircraft flying above the vicinity of coastal lines.

WDCGG provides ground-based CO_2 and CH_4 measurements. This dataset may well serve as collateral evidence if used with consideration given to seasonal variation and spatial representativeness. Among others, in the south hemisphere, where the seasonal variation of concentration is very small, this dataset is highly effective and may even serve as validation data.

One of possible scientific validation methods is to synthesize (or assimilate) the CO_2 distribution in the surrounding of the observation point based on the concentration profile measured by air-borne using regional atmospheric transport models, calculate the concentration profile up in the sky over the flat place with uniform albedo, which corresponds to the GOSAT observation point, and compare the findings with GOSAT product. However, the appropriateness of the method itself needs to be verified, first of all, and there are several other problems that remain to be addressed with this method.

The following sets forth policies concerning validation data collection.

- Install a number of observation instruments (high-resolution FTS, lidar and sky radiometer) at several specific observation points and perform observation with priority at these “focal observation points”.
- Effectively utilize “campaign observation with aircraft if necessary” for observation data on such meteorological and ground surface conditions that are not covered by the “focal observation points”.
- Utilize the observation data routinely acquired, such as those taken by the existing high-resolution FTS installed on the ground, air-borne observation data, and WMO WDCGG ground observation data, as the GOSAT observation coverage is the entire globe.
- The column abundances in sea areas are derived based on sunglint observation. As the concentration variation is smaller in sea areas than land areas, data covering the validation

sites on the ground that are located near the sea can be used with consideration given to the wind direction. Moreover, observation data acquired in islands and by vessels can also be used for indirect evaluation.

Based on the above policies, data at typical observation points are acquired; the specific criteria for selecting such observation points can be summarized as follows:

- Latitude: low , middle , high
- Amount of water vapor: high, low
- Albedo: uniform, nonuniform
- Aerosols: variant, invariant

At present, if 10 validation points for ground-based FTS observation and another 10 for aircraft observation can be acquired, minimum requirements in the validation can be satisfied. The total 20 are expected as sufficient to minimally cover the above conditions. However, if a handy validation observation instrument which satisfies the validation requirements is developed, more points may be selected and the validation can more largely be deployed.

Data measured at each observation point will be evaluated in light of both temporal and spatial variations to identify the uncertainties in the products. However, the evaluation of biases requires roughly three months at the sites where seasonal variation is small and six months in general. The evaluation results will be sorted according to the above criteria and quality will be assured by data category. In case that this approach is difficult, alternative effective methods include a trajectory analysis with consideration given to temporal and spatial variations and a validation analysis based on regional CO_2 transport models.

The following describes specific plans of observation and data acquisition for the validation purpose.

a) Validation by FTS observation

(i) Observation by ground-based high-resolution FTS

Observation by ground-based high-resolution FTS will be performed at several observation points in Japan, on the regular basis.

In conducting the validation, it is additionally useful that the observation data acquired by the ground-based high-resolution FTSs are analyzed and evaluated using the same data processing algorithm (radiative transport equation) as the one used for the analysis of TANSO-FTS.

(ii) Utilization of data acquired by ground-based high-resolution FTS networks etc.

Data from the ground-based high-resolution FTS observation networks will be used. The Project will also arrange the use of data at other observation points through direct negotiation with the pertinent data providers, RA-based joint researches, and so forth.

When selecting ground observational sites for the GOSAT validation, the most ideal sites at the initial validation stage should preferably have flat and uniform surface and extend for a wide range commensurate with the 10.5-km footprint of TANSO-FTS, whereby error factors can maximally be avoided.

Thus, the validation sites will be selected based on the following criteria.

- Seasonal variation: small (south hemisphere)→ large (north hemisphere)
- Air pollution: minor → major
- Land surface: simple → complex

The options are:

- Sunglint
- Snow and ice

(iii) Observation by small FTSs

If moving observation is necessitated, these small-sized FTS can be used, after evaluating the measurement accuracy, data quality and operational stability.

b) Validation by air-borne/balloon-borne observation

(i) Utilization of data from the air-borne observation

The continuous CO_2 measurement equipment on board aircraft acquires the spatial (horizontal) distribution of CO_2 concentration at very high altitudes and the vertical profiles CO_2 concentration around the airports, since it can acquire data while not only flying horizontally but also taking off (ascending) and landing (descending).

Additionally, as aircraft travels in the horizontal direction for approximately 100 km while ascending up to an altitude of about 10 km where it flies horizontally, and 200 to 300 km while descending from the stable altitude, spatial representativeness of the concentration should be taken into consideration at the time of analysis. To this end, transport models can be used for this evaluation. Furthermore, since the concentration in the lower atmosphere near the airport grows due to effects from the urban air in many cases, it is necessary to judge effectiveness of data in view of the wind direction. Moreover, the fluctuation of the CO_2 concentration in the layers above the highest altitude that the aircraft can reach must also be evaluated. So far, the findings from balloon-borne observation for the stratosphere have revealed that the fluctuation of the column abundance is around 0.5%, very roughly. More details will be investigated in continued studies to follow.

(ii) Data acquisition by balloons

Balloon-borne observation data, including the past data, must be obtained in order to ascertain the characteristics of the variation of the CO_2 column abundance in the layers above the upper limit of air-borne observation.

c) Others

(i) Observation by small balloons

The CO_2 sonde to be installed on board a small-sized balloon, which is being developed, may be used for the validation after evaluating the measurement accuracy, data quality and operational stability and ensuring that it is practical in terms of cost, etc.

(ii) Observation by compact spectrometer

Fabry-Perot Etalons based spectrometer, currently being developed, may be used for the validation after evaluating the measurement accuracy, data quality and operational stability and ensuring that it is practical in terms of cost, etc.

(2) Validation of CO_2 and CH_4 products by TIR observation

The data acquired for validating L2 SWIR CO_2 and CH_4 will also be used for validating L2 TIR CO_2 and CH_4 products. Additionally, the validation will be more effective if combined with air temperature, air pressure, humidity profile, and ground emissivity data. As for nighttime observation, the data already acquired will be utilized as far as possible. The validation plan will be further detailed in consultation with the parties responsible for TIR.

In addition, since air temperature and H_2O and O_3 concentration profile by TIR are products to be generated internally by JAXA for the research purpose, JAXA will carry out necessary evaluations on data quality.

(3) Comparison in the global distribution of CO_2 and CH_4 column abundances based on SWIR observation

L3 products do not require special evaluation since they are derived by temporal and spatial averaging of the validated L2 products.

(4) Comparison of CO_2 flux

The global distribution of L4A CO_2 flux and L4B CO_2 concentration are positioned as subject to comparison due to the following reasons, and it is preferred that these are evaluated as part of research activities, including RA, instead of validating in the Project.

- L4A and L4B are both calculated by models.
- The reliability of the transport models to be used is not firmly established and is still under discussion among scientists. Ensemble averaging among multiple models will enable a comparative evaluation.
- Flux observation is intended for the research purpose, and it requires substantial efforts to obtain the necessary data.
- The comparison of the flux observation with models requires scaling-up, which is a process still at the research level.
- The sea flux varies with the exchange coefficient.

L4A products provide an estimation of the monthly average of CO_2 flux in each of the 64 regions into which the globe has been divided.

As for comparison of L4A products with other observation data, data acquired by vessels are effective since the flux in sea area (latitude 5° × longitude 5°) is regarded as almost uniform.

On the contrary, the flux in land area is calculated based on the mesh size of latitude 1°× longitude 1° in the calculation process, in assumption of the flux distribution patterns within the regions. On the other hand, the ground-based observation of CO_2 flux is made on the “point” basis, with a significant regional difference and the smallness in number and spatial unevenness of the observation points, and thus it is difficult to use these points directly for the validation of L4A products. In order to solve this problem, a scaling-up method using land-area ecosystem models plays a vital role. Many countries, including Japan, have been engaged in research on such scaling-up methods and further progress in this effort is expected to be seen in the near future.

As for research on CO_2, the following comparisons can be conducted.

a) Use of data on the CO_2 flux between the air and the ocean

The CO_2 flux between the air and the ocean is calculated by measuring the partial pressures of CO_2 in the surface sea water and in the air and applying the exchange coefficient. The exchange coefficient depends on the wind velocity, temperature of water at the sea surface and salinity.

b) Use of the observation data acquired at flux monitoring sites

There are several flux monitoring sites in Hokkaido, and although there is a problem in the unevenness in topography and vegetation, the data obtained there by utilizing the land-area ecosystem model may possibly be used in comparison with the flux (L4A) in GOSAT global carbon balance estimation model.

(5) Comparison of the global distribution of CO_2 concentration

L4B products to be offered are a monthly average of 3D concentration distribution obtained as mesh data of latitude 1°× longitude 1°. The comparison of the L4B products with other observation data is made on the one-hour value or monthly average value of the latitude1°× longitude1° grid, which is the base data of the L4B products. As for the reference data, the data used as the reference in the L2 validation (column abundances acquired by the ground-based FTSs and concentration profile acquired by air-borne observation) and data acquired by several other kinds of ground and marine observations can be generally and comprehensively utilized.

(6) Comparison with other satellite data

Comparison with CO_2 and CH_4 column abundance data acquired by other satellites, such as the OCO, is instrumental for evaluation of the data quality of GOSAT products.

a) OCO

OCO is scheduled to be launched in December 2008 by NASA/JPL (Jet Propulsion Laboratory). It will observe the CO_2 column abundance in short wavelength-infrared bands, as with GOSAT. The satellite will fly at the forefront of the so-called A-train constellation of the U.S. EOS program and it can obtain necessary physical quantities, such as aerosols, from the other member satellites. Therefore, it focuses only on observation of the CO_2 (and O_2) column abundance.

OCO's spectrometer is a grating type and the observation bands are 1.61, 2.06 and 0.76 μm, which almost coincide with those of GOSAT's.

In the future, it is necessary to scrutinize the possibility of concluding a cooperative agreement or framework between the two missions and examine detailed methods of data acquisition and other procedures.

b) SCIAMACHY

SCIAMACHY (SCanning Imaging Absorption spectroMeter for Atmospheric CartograpHY)

is an on-board sensor of the ENVISAT of the ESA. Its primary purpose is to observe the atmospheric trace components necessary for chemistry in the troposphere and the stratosphere. The spectrometer is a grating type with eight channels sensitive to ultraviolet, visible, and short wavelength infrared bands. The observation modes range from nadir, solar/lunar occultation, and limb scattering. It observes both the concentration profiles and column abundances of O_3, CO, CH_4, etc.

In addition, as the derivation of CO_2 is also being attempted, it may serve as effective reference for comparison with the GOSAT data.

Even other satellites that are not originally intended to measure greenhouse gases, such as AIRS and IASI, can also be used as referential data sources.

B-2.4 Validation of parameters related to error factors in SWIR observation

(1) Aerosol, thin cirrus cloud

In order to evaluate the appropriateness of the L2 processing algorithm for TANSO-FTS (SWIR) data, the parameters related to error factors, namely the optical characteristics of aerosols, such as optical thickness, wavelength index, and single scattering albedo, and the vertical distribution, are extracted via the networks referred to hereunder or otherwise, in addition to the validation of data quality. It must be noted, however, that it takes a certain lead time for the latest data to be uploaded on the Website, and hence in case that it is urgent to obtain the data, a request for data acquisition must be made directly to the observer.

Furthermore, it is necessary to install sky radiometers and lidars at those locations where ground-based FTS or air-borne observation is carried out. The lidar can measure the vertical distribution of aerosols and thin cirrus clouds with an accuracy of approximately 15 m, and distinguish between sphericity and non-sphericity based on the extinction of polarization, thereby identifying whether the substance is rain cloud, cirrus cloud, or sand dust. The sky radiometer measures the direct solar irradiance and forward scattering in the sky. The measurements can also be used for estimating not only the optical thickness, particle size distribution, and complex refractive index, but also the single scattering albedo and phase function. These data are useful to the validation of TANSO-CAI products.

(2) Ground surface reflectance

The accuracy of the ground surface reflectance retrieved from SWIR data will be confirmed with the use of the following data. The observation points for this purpose must be selected where the land surface is homogeneous.

a) MODIS

MODIS (Moderate Resolution Imaging Spectroradiometer) is an optical sensor on board Terra and Aqua, NASA's earth observing satellites. It observes a wavelength range of 0.4 to 14 μm in 36 bands with a 2,330 km swath and spatial resolutions of 250 to 1,000 m. The Science Team at NASA developed the processing algorithms and each data center is generating various products including the ground surface reflectance.

b) ASTER

ASTER (Advanced Space-borne Thermal Emission and Reflection Radiometer) is an optical sensor on board Terra, NASA's earth observing satellite. It consists of the Visible Near-Infrared Radiometer (VNIR), Short-Wave Infrared Radiometer (SWIR) and Thermal Infrared Radiometer (TIR). It observes a wavelength range of 0.52 to 11.65 μm in 14 bands with a 60-km swath and spatial resolutions of 15 to 90 m. The standard products generated by the Japan side include the ground surface reflectance, land surface temperature, land surface emittance and DEM.

(3) Oxygen column abundance

The oxyten column abundance, obtained in Band 1(O_2 A band in 0.76 μm), will be validated.

a) Ground air pressure and rawinsonde data

The validation will be performed using the data routinely taken at observation points for the upper atmosphere together with new observation data to be acquired as necessary. The rawinsonde data will also be used for addional other validations.

b) Meteorogical data reanalysis

Since the observation points for thte upper atmosphere are not evenly distributed among the oceans, developing countries and polar areas, meteorogical reanalysis results are also used in the validation.

B-2.5 Validation of CAI Products

TANSO-CAI is a supplementary sensor to TANSO-FTS. In other words, the CAI products (concerning parameters related to error factors) that relates to the validation of TANSO-FTS L2 products should be validated with a priority because these CAI data are necessary for generating TANSO-FTS L2 products. On the other hand, the validation of the other CAI products is rated at a lower priority, while, in the meantime, the validation of cloud mask products is quite essential. CAI L1B products are generated by NIES, and the evaluation of the position, band-to-band registration, radiance, etc. is extremely important.

Since the CAI products and validation data of parameters related to error factors in short wavelength infrared are common in part, the detailed validation plan will be determined in coordination with the parties in charge of CAI.

B-2.6 Campaign Observation

Air-borne observation by the direct observation instrument is important to be performed simultaneously with observation by the remote sensing instruments, such as FTS, lidar or otherwise, in order to confirm the accuracy of TANSO-FTS measurements.

The evaluation will be performed as to whether temporal variation of the accuracy of each instrument is ascertained, by acquiring high-accuracy CO_2 concentration profile data by the aircraft which will ascend to a high altitude in synchronization with the satellite and calculating the column

abundance obtained therefrom. The CO_2 concentration above the highest altitude where the aircraft can reach varies with the altitude of the tropopause. Therefore, it is crucial to calculate the altitude of the tropopause correctly. To this end, interpolation of simultaneous observation data taken by the rawinsonde or meteorological reanalysis data is performed. It is also needed to measure the CO_2 concentration at the ground level, because the aircraft cannot measure the concentration between the land surface and the lowest altitude which the aircraft can observe.

Moreover, it is considered as effective to simultaneously carry out direct observation by aircraft on aerosols, which act as error factors.

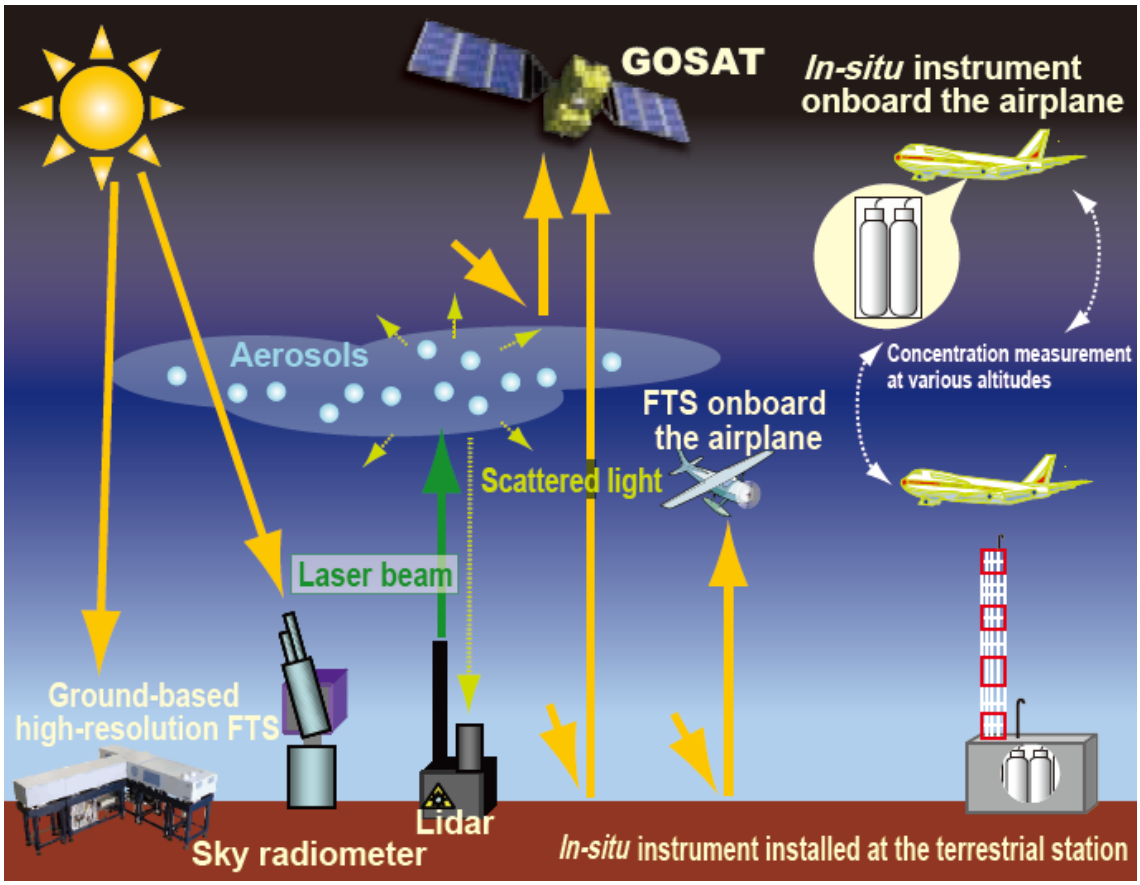

Figure B-2-1 Concept of the validation observation for CO_2 & CH_4 column abundances

B-2.7 Validation Schedule

Table B-2-1 lists the validation schedule based on the assumption that GOSAT will be launched January 2009.

This schedule is a plan for preparing the validation activities and securing the necessary data, as of the issuance of this document.

Table B-2-1 Validation Schedule

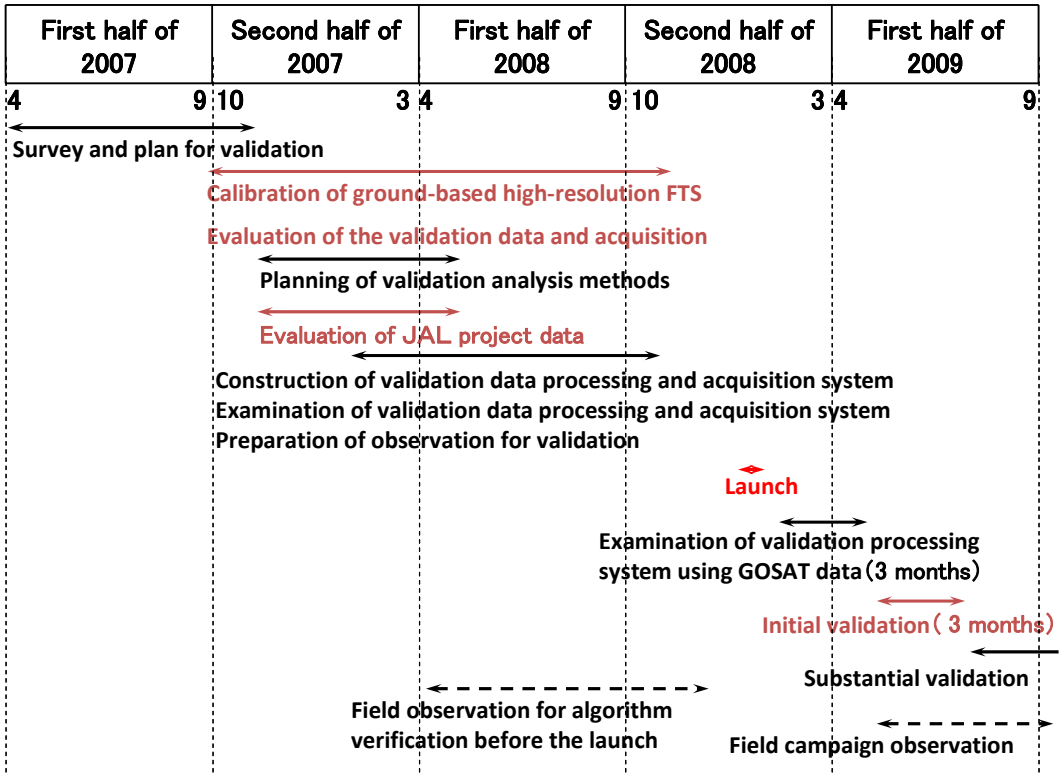

B-3 Overview of Processing Algorithms

This document describes processing flow and basic concepts of processing algorithms for GOSAT/TANSO data

B-3.1 Overview of the overall processing system

Figure B-3-1 shows an overview of the overall data processing flow together with the data level of the product produced at each step. More details of the processing levels (L1, L1A to L4B) of the GOSAT/TANSO data products are given in Table 1 of the RA Document.

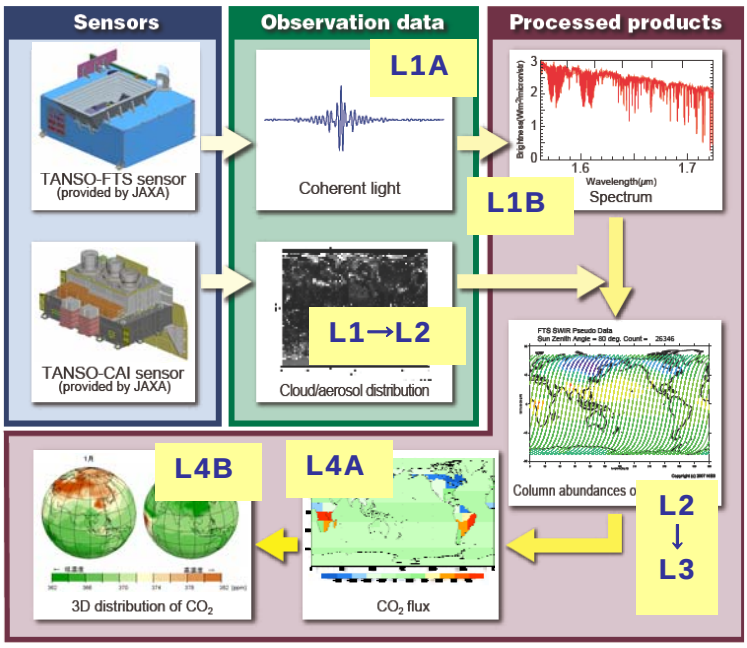

Figure B-3-1 Data processing flow and data product levels

The data measured with the TANSO-FTS and TANSO-CAI sensors are processed to several kinds of products according to the flow given in Fig. B-3-1. Interferograms (FTS L1A), observed values by FTS, are converted into spectra (FTS L1B), while the CAI L1 data are processed to cloud and aerosol properties (CAI L2). These data, at observation points under almost clear sky conditions, are combined to estimate the column abundances of CO_2 and CH_4 (FTS L2), and further to draw a global concentration map (FTS L3), and still further to estimate global carbon flux (emission and absorption) distribution (L4A) and three dimensional (3D) distribution of CO_2 (L4B) after analyses utilizing the atmospheric transport model.
The following sections of this Appendix outline the data processing steps and algorithms for the FTS and CAI data, focusing on L1 and L2 processing.

B-3.2 Level 1 processing of the TANSO-FTS data

(1) L1A data (interferogram)

L1A data consist of the interferograms of both observation data (the scattered light by earth-atmosphere system) and calibration data (the solar irradiation from outer space using the standard solar diffuser of the TANSO sensor), time data, mission telemetry data (temperature inside the instrument, pointing angle of the tracking mechanism, etc.), scale-conversion-related data, and so on. The L1A data, however, are regarded as "internal products", and will not be released to general users, but a part of them will be provided for the RA Investigators who research on themes in the field of calibration/validation or development of algorithms.

(2) L1B data (spectrum)

L1B data consist of basic data (number of datasets, gain value, scanning direction, etc.), spectra of observation data (voltage value per wave number [V/cm^{-1}]) for the short wavelength infrared "SWIR" bands, and spectral radiance [$W/cm^2/cm^{-1}/str$] for the thermal-infrared ("TIR") band), calibration data, instrument function, time data, mission telemetry data, scale-conversion coefficients, quality data, geometric information data (the latitude/longitude of the center of the observation point), and so on. Further, the calibration data on SWIR sensitivity will be provided.

(3) Overview of L1A to L1B processing

The data of the SWIR bands (Bands 1, 2, 3) are processed in the following steps.

- Engineering value conversion. (Conversion from discrete-valued digital numbers to voltage values)
- Spiky noises are detected and corrected. Basically, no non-linear correction is performed on the SWIR band data, though the correction function itself is equipped.
- The zero path difference (ZPD) position in the above interferogram is detected.
- Fourier-transformed.
- A flag is generated by confirming the low-frequency components in the spectrum. (A flag is set when the spectrum contains large values around the low-frequency region, to indicate that the FOV fluctuated and/or small vibration occurred during the scanning.)
- (In case that a flag is set) the interferogram is corrected by removing the low-frequency components of spectrum.
- By applying a given window function to decrease spectral resolution, the data are complex Fast-Fourier transformed (FFT) every 0.2 cm^{-1}. The phase angle is calculated from the ratio between real and imaginary parts after the transformation, while the phase information is derived from the transformed values.
- The interferogram is now zero-filled to yield 76,545 (= $3^7 \times 5 \times 7$) data points (after correction of the low-frequency components), complex Fourier-transformed without phase correction, and rotated by the phase angle derived from the above to produce the phase-corrected spectra (spectra of the real part). Note that the L1B data to be distributed will contain both real and imaginary parts.

The data of the TIR band (Band 4) are processed in the following steps. However, these steps represent just a method, and are subject to change in the future.

- Engineering value conversion. (Conversion from discrete-valued digital numbers to voltage

values)

- Spiky noises are detected and corrected, followed by non-linear correction after subtracting direct current (DC) components.
- The zero path difference (ZPD) position in the above interferogram is detected, FFT shifted.
- (Similarly to the SWIR data) the necessity for correction for the low-frequency components due to FOV fluctuation is checked from their spectrum without phase correction, and the correction is made if necessary.
- After the phase correction, the number of data points in the interferogram is adjusted to 38,400 (= $2^9 \times 3 \times 5^2$) through zero-filling, and the data are Fourier-transformed. Furthermore, by using the deep-space and blackbody observation data in the TIR band, observation spectral data (the real part data after Fourier-transformation) are converted into spectral radiance ($W/cm^2/cm^{-1}/str$).

As for Bands 1, 2, 3, if the interferogram exhibits a DN value of 65,400 or larger at the ZPD position, the data are regarded as saturated and a quality flag is set. As for Band 4, if the digital DN at the ZPD position is 65,400 or larger or 136 or smaller, the interferogram is regarded as saturated and a quality flag is set.

Moreover, the wavelength calibration is performed for the TANSO-FTS, due consideration to (i) the oscillation wavelength (1310 nm (nominal)) of the semiconductor laser varies with the temperature, and (ii) the alignment may be affected by the temperature variation in orbit.

B-3.3 Level 1 processing of the TANSO-CAI data

TANSO-CAI has four observation bands: Bands 1-3 have a wavelength width of 20 nm, spatial resolution of 0.5 km, and 2,000 elements, and Band 4 (the center wavelength is 1.60μm) has a wavelength width of 90 nm, spatial resolution of 1.5 km, and 500 elements.

L1A data are provided with information necessary for radiometric correction and geometric correction.

L1A data ,however, are classified as internal products of the Project, and will not be released to general users. However, some of them will be provided for the RA Investigators who carry out research on calibration/validation or development of algorithms.

(1) Radiometric correction

L1A digital data are converted into radiance values ($W/m^2/\mu m/str$), using scale conversion coefficients. Since the detectors are of diode type, it is, in principle, not necessary to perform non-linear correction of the output values. In addition, the gain setting for the CAI observation bands will be adjusted, based on the gain switch table to be generated on the monthly basis, so as to avoid saturation of output signals.

(2) Geometric correction

Information on the relative scales (expansion, compression and rotation) for datasets of different

bands makes it possible to determine the band-to-band registration. By making Band 3 the reference, other bands' data are expressed relatively as the displacement from the reference. The number of center pixels for Bands 1-3 is 1,024, and that for Band 4, 256, and the band-to-band registration error after correction is targeted at 0.2 pixel or lower. In addition, L1 data are supplemented with the latitude and longitude information of the representative elements.

(3) L1B data
TANSO-CAI L1 data are supplemented with the above-mentioned information necessary for correction before release. L1B data are generated as standard products with the observation positions corrected, after scale conversion based on the information, band-to-band registration, and ortho-rectification per pixel based on the elevation information (Digital Elevation Model: DEM).

(4) L1B+ data
CAI L1B data are then projected on a map, on a certain scene scale, and their stored radiance data per pixel/band are resampled to generate L1B+ image data (standard products) for release.

B-3.4 Level 2 processing of the TANSO-CAI data

The CAI data are processed to standard products which provide cloud flag information. Research products, which provide parameters of cloud and aerosol characteristics, are derived from these products.

First of all, optically thick clouds on the sea surface and on relatively dark land surfaces are discriminated by using two visible bands of the CAI sensor. If they are found to be clouds, specifically water clouds, cloud characteristics are analyzed. The cloud characteristics to be estimated are the cloud optical thickness (at a wavelength of 0.5μm) τ_c, which is a non-dimensional value that represents the optical thickness of clouds, and the effective radius of a cloud particle τ_e. Table B-3.4-1 lists up the cloud products to be derived from the CAI data.

Table B-3.4-1 Cloud products derived from the CAI sensor

Estimated parameter	Unit	Band No.	Remarks
Cloud flag	-	2, 3, 4*	Optically thick clouds on the sea surface and relatively dark land surface
Cloud optical thickness (@0.5μm)	-	2, 4	Water clouds and ice clouds
Effective radius of cloud particles	μm	2, 4	Water clouds and ice clouds
Vertically integrated total amount of cloud water	g/m^2	2, 4	

* Band 4 will be used for studies.

Secondly, aerosol characteristics are analyzed by combining data from all CAI observation bands with ancillary data, including meteorological data. There are various types of aerosols existing on the globe; the primary aerosols include anthropogenic aerosols, such as sulfates, black carbons, and organic carbons, and dust aerosols and sea salt aerosols. In estimating the aerosol characteristics, it is assumed that anthropogenic aerosols are composed of internal mixing of sulfates and black carbons, and the three types of aerosols, i.e. anthropogenic, dust, and sea salt aerosols, are mixed externally to constitute a particle system. Based on these assumptions, the optical thickness of each type of aerosol (at a wavelength of 550nm), τ_a, and the component ratio (volumetric ratio) of black carbon to anthropogenic aerosols, γ_{soot} will be estimated. These are summarized in Table B-3, 4-2.

Table B-3.4-2 Aerosol parameters estimated from the CAI data

Estimated parameters		
Aerosol optical thickness (Wavelength: 550nm)	Anthropogenic aerosol mode	τ_{acm}
	Dust aerosol mode	τ_{dst}
	Sea-salt aerosol mode (over the sea only)*	τ_{slt}
Volumetric ratio of black carbons in the anthropogenic aerosol mode		v_{soot}

*Except sunglint region

The following provides an outline of individual processing algorithms.

(1) Cloud flag algorithm

Multi-wavelength imagers, such as MODIS and GLI, have water vapor channels and infrared split windows to discriminate altostratus and cirrus, in addition to many visible channels, and thus can accurately discriminate clouds as a single sensor. In contrast, the CAI sensor has only four bands with a wavelength range of near-ultraviolet to short wavelength infrared, making its discrimination accuracy potentially inferior to MODIS or GLI. For this reason, users of cloud flags are recommended to appropriately select and employ the several types of cloud discrimination test

results provided by CAI and the cloud flags provided separately by FTS observations and others. Of the CAI observation bands, Band 2 (0.670μm) and Band 3 (0.865μm) are the primary bands for discriminating clouds. Although it is possible to use the short wavelength infrared 1.6μm band (Band 4) to discriminate between ice clouds and water clouds in the presence of optically thick clouds, this is currently at the examination stage. Two types of threshold-value tests are currently planned using the cloud flag algorithm: tests to examine the reflectances in visible bands 2 and 3 and a color test for the ratio of the reflectances between these two bands. The former is a discrimination method that utilizes the fact that the reflectance on clouds is higher than that on the sea surface or on relatively dark land surfaces, while the latter stands on the fact that the reflectances on clouds in Bands 2 and 3 are almost equal.

The CAI cloud flag algorithm will be used to conduct the four tests listed in Table B-3.4-3 below, and the test results will be stored as data.

Table B-3.4-3 CAI cloud flag tests (Draft)

Test No.	Contents to be implemented
Test 1	R[B2] > (R2+A[B2])
Test 2	R[B3] > (R3+A[B3])
Test 3	0.9 < (R[B2]/R[B3]) < 1.1
Test 4	If “true” on Test 1 and Test 3, examine R[B4]/R[B2].

Here, R[B2], R[B3], and R[B4] represent the reflectance in CAI Bands 2, 3, and 4[Note 1)], respectively; A[B2] and A[B3] represent the ground-surface albedo in Bands 2 and 3; and R2 and R3 are the margin values of the ground-surface albedo. Tests 1 to 3 diagnose the possibility that object pixels are clouds. The results of Test 4 provide information conducive to discriminating between ice clouds and water clouds, on an examination basis. The accuracy of cloud flag achieved by the CAI sensor alone may be subject to the following limitations: Optically thin clouds, particularly cirrus, cannot be completely identified by this method; and discrimination of clouds by CAI is limited on bright ground surfaces, such as surfaces covered with snow and ice or desert, and in regions where the ground surface state changes rapidly with time.

Note 1) The reflectance is defined as $\pi L/(F_0 \cos\theta_0)$ here. L is observed radiance, F_0 is solar irradiance based on the instrument function, and θ_0 is the solar zenith angle.

(2) Cloud characteristics algorithm

The principle for obtaining optical thickness of the cloud and effective radius of cloud particles are as follows. Light is scarcely absorbed in CAI Band 2 (0.670μm) even if multiple scattering by cloud particles occurs since the imaginary part of the complex index of refraction of water droplets is very small and is approx. 10^{-8}. Therefore, the light injected into the cloud layer repeats scattering due to cloud particles and ultimately the light that scatters toward the satellite from the top of the cloud is observed. A greater amount of light is observed in CAI Band 2 as the cloud optical thickness increases, augmenting the light scattered upward from the top of the cloud. The probability of upward scattering as a result of multiple scattering will reach the upper limit when the optical thickness increases to around 70, and the observed radiance will be saturated in the meantime.

On the other hand, CAI Band 4 (1.6μm) is used to estimate the effective radius of cloud particles. The imaginary part of the complex index of refraction of water droplets in this wavelength range is over 10^{-5}, which is one thousand times greater than that in visible light. Therefore, the short wavelength infrared light that enters the cloud layer is absorbed during the multiple scattering due to cloud particles. The light observed by the CAI Band 4 gets weaker, when cloud particles become larger and therefore absorb light more strongly. The absorption in the cloud layer becomes gradually saturated when the effective radii of cloud particles increase to around 30μm, which is the upper limit.

In remote sensing of cloud characteristics, the optical thickness and effective radius of particles of clouds are calculated from observed radiances in visible and infrared bands. The radiances directly observed include radiative components that are essentially unnecessary for estimation of clouds characteristics, such as the ground surface reflection components and thermal radiation components from the cloud layer. These components are therefore removed in calculation by using the transmittance of the atmosphere and cloud, satellite zenith angle, solar zenith angle, relative azimuth angle, etc. Estimations of the physical values using satellite observations are accomplished by comparing the simulated radiance obtained by using the radiative transfer code (Nakajima and Tanaka, 1986, 1988) and the observed radiances by CAI. A database (lookup table, LUT) table of angle dependent radiance, transmittance of atmosphere and cloud, and spherical albedo has been prepared in advance for various optical thickness of cloud and the effective radius of cloud particles, and it is used in this algorithm which performs iterative calculations using the Newtonian method.

(3) Aerosol characteristics algorithm

CAI has observation bands at 670 nm and 870 nm, which are sensitive to aerosol scattering and often utilized for remote sensing of aerosols, as well as the band at 380 nm, which is insensitive to reflection from the ground surface and sensitive to absorptive aerosol, and the band at 1.6 μm, which is sensitive to large-particle aerosols. The aerosol characteristic parameters will be estimated by the maximum a posteriori (MAP) method, calculating the satellite signals of these four bands theoretically.

In addition, as the estimation of aerosol parameters based on the CAI data is tightly restricted, aerosol information on the locations which are not covered by CAI estimation will be obtained from the estimation results based on the aerosol transport model being developed by the GOSAT Project. This model is a 3D dynamic simulator for aerosols developed for the GOSAT Project, having Spectral Radiation-Transport Model for Aerosol Species (SPRINTARS) as its core.

B-3.5 Level 2 processing of the TANSO-FTS-SWIR data

In the three FTS SWIR bands, the sensor observes signals on the two polarization planes, which are perpendicular to each other, in each band. That is, it acquires data (interferogram) for six bands, in total. The FTS SWIR data, combined with various ancillary data, are used to calculate the column abundances of CO_2 and CH_4 within target accuracies (i.e. relative errors of 1% for CO_2 and 2% for

CH_4 in a certain period). The retrieved column abundance [molecules/cm^2] is converted to XCO_2 [v/v] (volumetric mixing ratio), which represents the ratio of CO_2 in the atmosphere with no water vapor, or a relative humidity of 0%, (dry atmosphere). In many cases it is this converted quantity that is used for application. This conversion requires ground-surface pressure information, thus the column abundance of oxygen (or ground-surface pressure) derived from FTS Band 1 data and the ground-surface pressure obtained from objective analysis data at the observation time and location are used.

Figure B-3-2 on the next page depicts the data processing flow for generating L2 column abundance products from L1B (spectra) data of FTS SWIR observation.

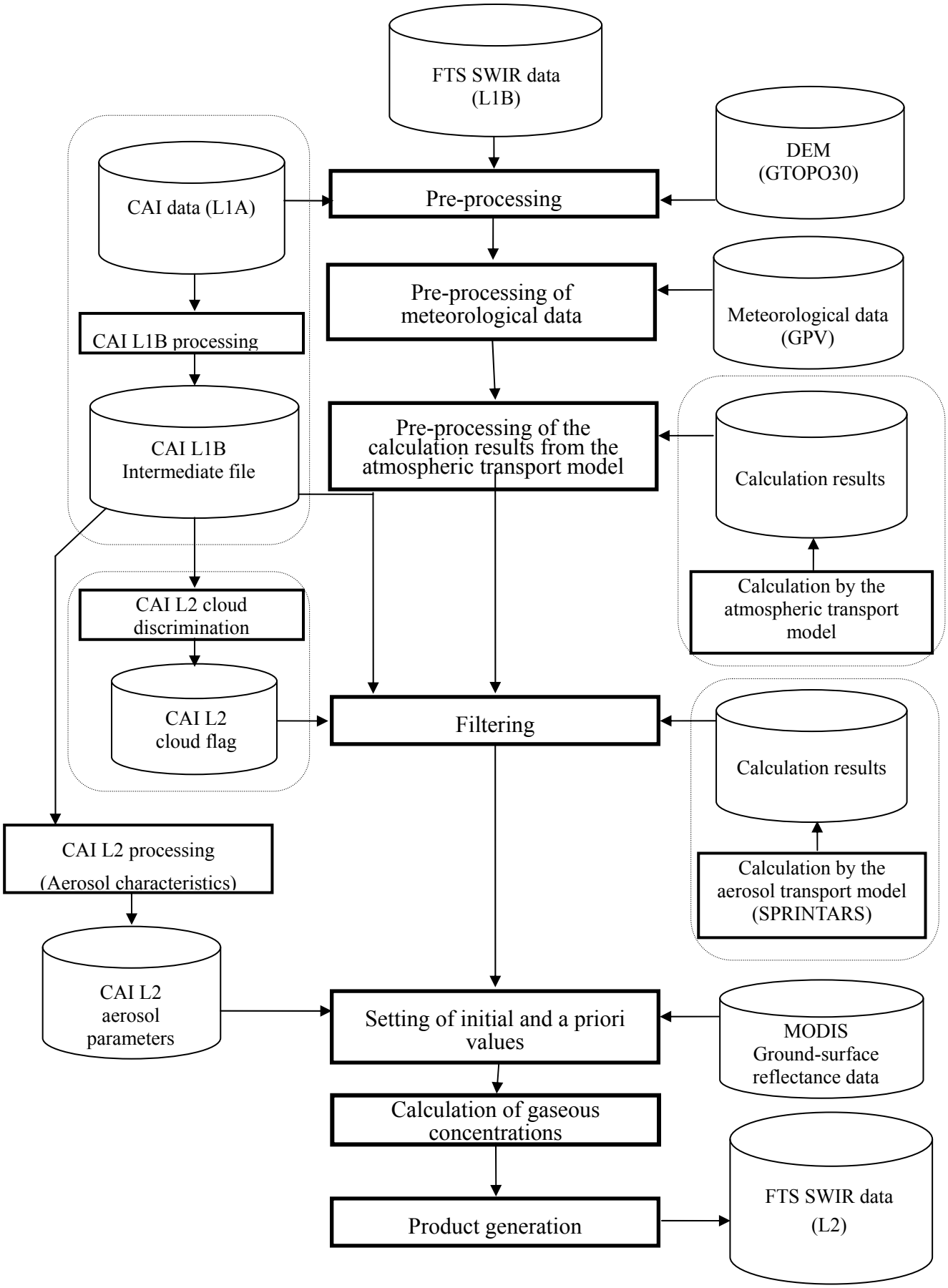

Figure B-3-2 Data processing flow from TNASO-FTS-SWIR L1B to L2 products

(1) Use of polarization information

The FTS SWIR observation can measure polarization signals on two perpendicular axes, which are called the P (parallel) axis and the S (senkrecht—a German word for "perpendicular") axis. The P and S observation data are planned to be applied in the data processing flow, by means of the following three approaches. "Approach 1" will be adopted in the initial version of the processing algorithm. A series of simulations have found that the degree of polarization is low in observation of reflection from the earth surface, whereas it is high in sunglint observation over the sea surface.

【Approach 1】 The two polarization components of the observed light are compounded to provide total intensities. In this approach, the scalar radiative transfer code, which does not take the polarization state into consideration, will be used in the theoretical calculation.

【Approach 2】 The radiance spectra of the two polarization components of the observed light are used independently. In this approach, the vector radiative transfer model (Pstar2b code), developed by the GOSAT Project, will be used in the theoretical calculation. The Pstar2b code runs at a speed a few times slower than conventional scalar radiative transfer codes, however, it is a code which runs much faster than any other polarization calculation code, after being improved for fast running.

【Approach 3】 The radiance spectra of the two polarization components of the observed light are approximated by total intensities. In this approach, it is assumed that polarization-related parameters, such as ground-surface albedo, scattering phase matrix, etc., are different between the two polarization components, whereas the other parameters, including the optical thickness and gaseous concentration, are identical. Based on these assumptions, the radiative transfer is calculated in an approximate manner, using a scalar radiative transfer code per polarization axis.

(2) Retrieval algorithm

In the processing algorithm to estimate column abundances from L1B to L2, the first calculation is for the vertical distribution of the volumetric mixing ratio of the gas of interest as an intermediate parameter, in preparation for achieving the column abundances of CO_2 and CH_4 as final outputs. The information necessary for this retrieval will be supplied by objective analysis data for the meteorological parameters, such as the vertical distributions of air temperature and pressure, measured at the same location at the same time as the GOSAT observation. In addition, absorption bands in the FTS SWIR bands do not have such radiance spectral signals that have a weighting function structure which is steep enough in the altitude direction to require vertical distribution. Therefore, the intermediate product, the vertical distribution of the volumetric mixing ratio, may have an extremely unstable structure. Nevertheless, the column abundance can be stably obtained. The reason is, though the explanation is not rigorous as it disregards the impact of multiple scattering or path radiances, that the size of the area obtained by integrating the absorption depth of the absorption line structure within the radiance spectrum observed is deeply linked with the amount of column abundance.

The L1B to L2 retrieval algorithm is based on a constrained Gauss-Newton method of a

non-linear least squares method to the observed radiance spectra. In other words, the solutions are obtained stably from the observation information together with a priori information. The solutions to be derived consecutively are expressed as the following equation.

$$x_{i+1} = x_i + \left(K_i^T S_\varepsilon^{-1} K_i + S_a^{-1}\right)^{-1} \left[K_i^T S_\varepsilon^{-1}\left(y - F(x_i)\right) - S_a^{-1}\left(x_i - x_a\right)\right] \qquad \text{B-3-(1)}$$

Where x_i is the vector of the parameter to be estimated at the i^{th} time, x_a is its a priori information (the a priori value which can be used as the initial guess at the beginning of estimation), S_ε is the error variance-covariance matrix (no. of wavenumber points × no. of wavenumber points) of the observed spectra, S_a is the variance-covariance matrix (no. of parameters to be estimated × no. of parameters to be estimated) of the a priori information, y is the vector of observed spectrum (no. of wavenumber points), $F(x_i)$ is the simulated spectrum theoretically calculated using a radiative transfer code when the variable is x_i, and K_i is the Jacobian matrix (no. of wavenumber points × no. of parameters to be estimated), which expresses the divergence of spectra against the unit change of the target parameter. Note also that $K = \partial y / \partial x$ here.

Furthermore, Equation B-3-(1) above corresponds to an adoption of such a solution that gives the minimum value for the cost function given as below (Equation B-3-(2)). It is called the Maximum A Posteriori (MAP) estimation method.

$$J(x) = \left[y - F(x)\right]^T S_\varepsilon^{-1} \left[y - F(x)\right] + \left(x - x_a\right)^T S_a^{-1} \left(x - x_a\right) \to \min. \qquad \text{B-3-(2)}$$

The values of elements of S_ε will be determined based on the characteristics of the sensor (e.g. SNR). The values of the diagonal elements of S_a are given by a priori information regarding how freely the target parameters can vary with altitudes, while those of the non-diagonal elements are given by the information regarding the inter-constraints of variation among the target parameters (e.g., correlation between vertical distributions of each gaseous species).

Basically, the molecular spectroscopic parameters provided by the HITRAN 2004 database will be used for calculating theoretical spectra in B-3-(2), except CO_2 of Bands 2 and 3 and partly CH_4 of the 1.67-μm band, for which the 2008 version of line parameters and data generated in the GOSAT Project will be used, respectively. Moreover, when performing spectral-fitting in B-3-(2), channel selection will be performed in order to eliminate the impact of Fraunhofer lines in the solar atmosphere and of water vapor in the earth atmosphere. The information on solar Fraunhofer lines in the 1.6-μm and 2.0-μm bands will be supplied by the data generated by Dr. R. L. Kurucz, Harvard-Smithonian Observatory in the U.S., in response to the request from the GOSAT Project.

Research and development of this algorithm have been promoted using the radiative transfer code improved based on HSTAR code, an extended RSTAR code developed by Professor Teruyuki Nakajima and his research group at Center for Climate System Research, University of Tokyo, which can calculate the effects of (multiple) scattering and attenuation by atmospheric

molecules, aerosol, and clouds particles present on the optical paths. With the help of this code, the column abundance can be estimated at an expected precision even in the presence of optically-thin clouds and aerosols, as demonstrated in numerical simulations. Consequently, the "filtering" process in the processing flow provided in Figure B-3-2 is the process carried out by the program to determine whether or not the observation data under processing is a clear-sky scene or a scene with optically-thin clouds or aerosols. The data processed in this way then undergo L2 processing.

In addition, the ground-surface albedo is also added as a target parameter and retrieved simultaneously by means of Equation B-3-(1). With this processing, it is possible to flexibly estimate the column abundances of CO_2 and CH_4 for any spectrum structure of the ground-surface albedo.

(3) Fast retrieval algorithm

In order to realize the above-mentioned estimation algorithm, a new data processing system which combines the discrete ordinate method as a radiative transfer and the MAP method, is being developed. Additionally, the Project is promoting the research and development on a fast and high-accuracy technique called the Photon Path-length Probability Density Function (PPDF) method, which is based on a simple radiation model by combining the Monte Carlo method and the Equivalence theorem and retrieves PPDF parameters simultaneously with other unknown quantities, such as CO_2, from the observed spectra, as a future version of GOSAT operational processing algorithm.

B-3.6 Level 2 processing of the TANSO-FTS (thermal-infrared band) data

Data from thermal-infrared sensors on board spacecraft platforms have been used mainly for analyzing CO_2 concentrations. With this technique, however, it is difficult to detect significant change in the CO_2 concentration in the boundary layer, such as decrease due to absorption by vegetation or increase due to artificial CO_2 sources, although the changes in concentration in the middle and upper layers of the troposphere can be analyzed with a high accuracy. This is because the difference between the atmospheric temperature at the altitude where concentration changes occur and the equivalent radiance temperature of the background radiation is smaller in the lower layers of the atmosphere, making it more difficult to detect.

For FTS thermal-infrared observation (referred to as "TANSO-FTS-TIR" hereafter), it is expected that the vertical profile of CO_2 concentrations down to altitudes of 700 to 750 hPa from the upper atmosphere can be obtained under clear-sky conditions, though it depends on the vertical profile of atmospheric temperatures. Figure B-3-3 plots a typical vertical resolution function (Averaging Kernel) in medium latitudes.

(1) Vertical profile of CO_2 concentrations

Independent temperature information is required for deriving the concentrations of CO_2 from the thermal-infrared band data. The TANSO-FTS TIR observation uses objective analysis data because there are no simultaneously-operated microwave sensors.

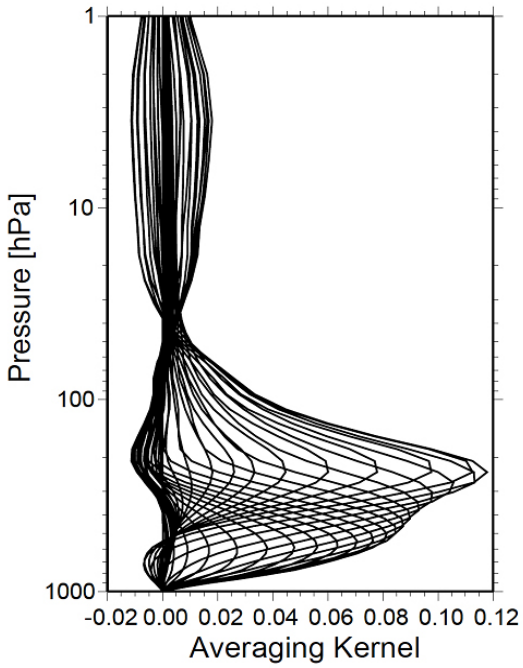

Figure B-3-3 Averaging kernel of CO_2 analysis based on the TANSO-FTS-TIR data -Typical example in mid- latitudes (Saitoh et al., 2006)

For retrieval analysis of CO_2 concentrations, a physical analysis technique, more precisely the Maximum A Posteriori (MAP) method as in Eq.B-3-(2), will be employed, similarly to FTS SWIR observation.

The results obtained by statistically processing the output of the CO_2 transport model will be used as the initial guess values and covariance values of the CO_2 concentration. Since the Jacobian matrix is a function of vertical profiles of atmospheric temperatures and CO_2 concentrations, the optimal Jacobian matrix is calculated for each region, season, and local time from the vertical profiles of atmospheric temperature and CO_2 concentration from the objective analysis and the above-mentioned initial guess value, respectively.

(2) CO_2 column abundance

The radiance spectrum of the CO_2 hot band close to 10 μm is utilized for this analysis; namely, the fact is used that the decrease in radiance depends on the column abundance of CO_2 with the background of a warm ground surface or sea surface as in Solar Occultation.

First, the Jacobian matrix in the 10 μm band of CO_2 is calculated based on the vertical profiles of atmospheric temperatures and volumes of water vapor in each FTS FOV that was analyzed using the objective analysis value as the initial guess value. To reduce errors in estimating the volume of water vapor, baseline compensation is performed such that the systemic gap between the simulated spectrum and the observed spectrum is compensated using a wavelength range with a small volume of absorption by gases. The column abundance of CO_2 is derived by applying the Jacobian matrix

to the difference between the simulated spectrum and the observed spectrum after this baseline compensation. The wavelength dependence of the ground-surface emissivity is required to simulate the radiance spectrum; the results estimated from database for the ground-surface emissivity and the meteorological data obtained before and after the observation are utilized for such data. For the concentration of ozone, which influences this wavelength band, data of other satellite sensors such as OMI, are utilized.

(3) Cloud screening

The fractional cloud coverage in the FTS FOV is estimated based on the analysis results of the CAI sensor during the daytime. However, the analysis results of the FTS TIR data are also used concurrently because thermal infrared radiation spectra are superior in detecting thin ice clouds such as cirrus clouds. During the nighttime, however, clouds are discriminated solely by the FTS TIR band because the CAI sensor is not operated.

There are three methods for analyzing clouds using the FTS thermal-infrared data.

1. Slicing method
2. Threshold value method
3. Split window method

The slicing method estimates the altitude at the top of cumulus clouds by applying the method of Menzel et al. (1983), which uses the 15 μm band of CO_2. The threshold value method, the second item above, discriminates clouds based on the difference between the value provided by the sea-surface temperature database, storing the analyzed results of data from the AVHRR on NOAA satellite and/or MODIS, and the sea-surface temperature estimated from the FTS TIR data with the assumption of no cloud. Although this method is superior over the sea, these data will be used only as references for land areas due to a large error in the ground-surface temperature of objective analysis data. The split window method, listed last, performs an analysis using the combination of data of two wavelength bands, 8 to 10 μm and 11 to 13 μm, which enables to judge cloud altitudes and distinguish between ice and water particles in the areas that are identified as cloudy.

B-3.7 Level 3 processing and more advanced (higher-level) processing

L3 product is generated as a global map, by using the column abundances of CO_2 and CH_4 (L2) calculated from the TANSO-FTS-SWIR data after applying temporal/spatial interpolation and appropriate statistical processes to the GOSAT observation data for fixed sections (e.g. 2.5° meshes (TBD)) during a given period of time, to calculate the value for each section. Similarly, TIR L3 product is planned as a global map, but the details are yet to be determined.

L3 processing of the CAI data is also planned, though very roughly, to provide standard products on global radiance maps (with cloud cover), global radiance maps (without cloud cover), and vegetation index maps (for a certain observation period), and research products on aerosol characteristics maps and cloud characteristics maps (for a certain observation period) . Details will be fixed hereafter.

More advanced-level products are also planned, targeting the release just after one year, at the shortest, after the satellite launch. These include global flux maps (L4A) in 64 divided regions,

which will be generated through inverse calculation, based on atmospheric transport models ,of GOSAT L2 or L3 data and CO_2 and CH_4 concentration data acquired at monitoring stations on the ground , and 3D distribution maps of CO_2 and CH_4 concentrations (L4B) calculated from L4A data using atmospheric transport models. The details of processing algorithms for these products have not been finalized yet, and hence are excluded from this Appendix.